



Characterization of Age-Related Differences in the Human Choroid Plexus Volume, Microstructural Integrity, and Blood Perfusion Using Multiparameter Magnetic Resonance Imaging

Joseph S. R. Alisch, Matthew Kiely, Curtis Triebswetter, Maryam H. Alsameen, Zhaoyuan Gong, Nikkita Khattar, Josephine M. Egan and Mustapha Bouhrara*

Laboratory of Clinical Investigation, National Institute on Aging, National Institutes of Health, Baltimore, MD, United States

OPEN ACCESS

Edited by:

Zhen Zhao,
University of Southern California,
United States

Reviewed by:

Danny J. J. Wang,
University of Southern California,
United States
Xiaodan Liu,
University of Southern California,
United States

*Correspondence:

Mustapha Bouhrara
bouhraram@mail.nih.gov

Received: 01 July 2021

Accepted: 30 August 2021

Published: 17 September 2021

Citation:

Alisch JSR, Kiely M, Triebswetter C, Alsameen MH, Gong Z, Khattar N, Egan JM and Bouhrara M (2021) Characterization of Age-Related Differences in the Human Choroid Plexus Volume, Microstructural Integrity, and Blood Perfusion Using Multiparameter Magnetic Resonance Imaging. *Front. Aging Neurosci.* 13:734992. doi: 10.3389/fnagi.2021.734992

The choroid plexus (CP) is an important cerebral structure involved in cerebrospinal fluid production and transport of solutes into the brain. Recent studies have uncovered the involvement of the CP in neurological disorders such as Alzheimer's disease and multiple sclerosis. However, our understanding of human age-related microstructural and functional changes in the CP with aging and neuropathology is limited. In this cross-sectional study, we investigated age and sex differences in the CP structure and function using advanced quantitative magnetic resonance imaging methodology in a large cohort ($n = 155$) of cognitively unimpaired individuals over a wide age range between 21 and 94 years. Our analysis included volumetric measurements, relaxometry measures (T_1 and T_2), diffusion tensor imaging (DTI) measures of fractional anisotropy (FA) and mean diffusivity (MD), as well as measures of cerebral blood flow (CBF). Our results revealed that CP volume was increasing with advancing age. We conjecture that this novel observation is likely attributed to alterations in the CP microstructure or function as well as to ventriculomegaly. Indeed, we also found that CBF was lower with advanced age, while, consistent with previous studies, T_1 , T_2 and MD were higher, and FA was lower with advanced age. We attribute these functional and microstructural differences to a deteriorated CP structural integrity with aging. Furthermore, our relaxometry and DTI measures were found to be associated with differences in blood perfusion revealing lower microstructural integrity with lower CBF. Finally, in agreement with literature, sex-related differences in MD and CBF were statistically significant. This work lays the foundation for ongoing investigation of the involvement of CP in neurodegeneration.

Keywords: choroid plexus, aging, magnetic resonance imaging, relaxometry mapping, diffusion tensor imaging (DTI)

INTRODUCTION

The choroid plexus (CP) modulates brain homeostasis through several processes including cerebral spinal fluid (CSF) secretion and expression of various proteins (Lun et al., 2015; Hofman and Chen, 2016). Specifically, the CP secretes numerous neurotrophic factors implicated in neurogenesis, vascularity regulation, maintenance of brain function, and signaling molecules including neuroinflammatory cytokines (Arnaud and Di Nardo, 2016; Mazucanti et al., 2019). The ubiquitous multifunctional role of the CP was highlighted in a recent study by Mazucanti et al. (2019), indicating that insulin is produced in the CP and modulated by serotonin. Structurally, the CP is a monolayer of epithelial cells connected by tight junctions situated within the ventricles that regulate the passage of solutes, proteins, and inflammatory cells to and from the CSF (Lun et al., 2015). Fenestrated capillaries are separated from the epithelial cells by stroma, and allow filtration of fluids, thereby forming the blood-CSF-barrier (BCSFB) (Liddelow, 2015).

According primarily to postmortem and animal studies, during normal aging, the CP undergoes several alterations, including morphological changes to the epithelial cells (Shuangshoti and Netsky, 1970; Serot et al., 1997, 2001; Marques et al., 2013), accumulation of calcifications (Yalcin et al., 2016), increased T helper type 2 (Th2) response (Baruch et al., 2013), dysfunction in CSF production and clearance (May et al., 1990; Chiu et al., 2012), and iron deposition (Joseph-Mathurin et al., 2013). Moreover, the CP is highly vascularized and contains energy-demanding epithelial cells, rendering it vulnerable to hypoxia, ischemia and hypoperfusion, potentially leading to cell death, increased permeability and dysfunction of the BCSFB (Chen et al., 2009), and reduced secretion of trophic factors and CSF generation. These changes have been associated with neurodegenerative diseases including Alzheimer's disease (AD) (Kadel et al., 1990; Cornford et al., 1997; Ennis and Keep, 2006; Krzyzanowska and Carro, 2012; Marques et al., 2013; Kaur et al., 2016; Hubert et al., 2019). The CP is a small region and difficult to distinguish from the surrounding tissue, requiring high resolution imaging and careful postprocessing manipulation including CP volume segmentation; therefore, despite its mediation of several critical processes, the effect of normal aging on CP microstructure and perfusion has not been well studied *in-vivo* in humans.

Previous magnetic resonance imaging (MRI)-based studies have demonstrated that subjects with psychiatric disorders (Lizano et al., 2019), complex regional pain syndrome (Zhou et al., 2015), multiple sclerosis (Ricigliano et al., 2021) and stroke (Egorova et al., 2019), have larger CP volumes compared to healthy controls, whereas studies evaluating CP size in participants without any sign of pathology have only looked at thickness. Indeed, although Madhukar et al. (2012) and İmamoglu et al. (2013) showed that CP thickness was consistent in pediatric and adult cohorts, changes in CP volume in normal aging has not been characterized. Moreover, to the best of our knowledge, MRI-based microstructural and perfusion differences in the CP with age or sex have only been documented by two studies. In this pioneering work, Alicioglu et al. (2017) assessed

the mean diffusivity (MD), measured using diffusion tensor imaging (DTI) MRI, in human CP across various age ranges and found that the eldest participants exhibit significantly higher MD than the younger participants; this result was interpreted as an increase in diffusion in CP with age indicating a loss of structural integrity resulting in increased leakiness of the epithelial cell junctions. In contrast, Bouzerar et al. (2013) reported a decrease in capillary permeability with age. Additionally, the authors observed no significant difference in CP CBF with age using dynamic susceptibility contrast enhanced MRI (Bouzerar et al., 2013). The discrepancy in results may be due to cerebral lesions present in patient data or the limited age range or size of the cohorts studied.

Several quantitative MRI techniques have been used to evaluate cerebral tissue microstructure *in-vivo* with aging and neuropathology (Grieve et al., 2007; Hasan et al., 2010; Alisch et al., 2021). Longitudinal and transverse relaxation times (T_1 and T_2) depend on water mobility as well as macromolecular tissue composition including iron content; therefore, changes in T_1 or T_2 are directly associated with cerebral microstructural tissue changes (Deoni, 2010). Further, fractional anisotropy (FA) and MD, derived from DTI, can be used to probe cerebral tissue microstructural integrity based on water content and mobility (Alexander et al., 2007; Grech-Sollars et al., 2015). Finally, cerebral blood flow (CBF) in the CP can be reliably determined using arterial-spin labeling (ASL) MR imaging (Evans et al., 2020; Zhao et al., 2020). In the current study, we investigated volumetric differences with age as well as microstructural and perfusion characteristics of the CP in a large cohort of well-characterized cognitively unimpaired adults ($n = 155$) across the extended age range of 21–94 years. Our main goals were to investigate the effect of age and sex on relaxation times, DTI indices and CBF, to investigate the effect of age and sex on CP microstructure and function, and to develop further insights into CP maturation and degeneration with aging.

MATERIALS AND METHODS

Participants

The MRI protocol was approved by the MedStar Research Institute and the National Institutes of Health Intramural Ethics Committees, and all examinations were performed in compliance with the standards established by the National Institutes of Health Institutional Review Board. Participants were drawn from the Baltimore Longitudinal Study of Aging (BLSA) (Shock, 1984; Ferrucci, 2008), and the Genetic and Epigenetic Signatures of Translational Aging Laboratory Testing (GESTALT) study. The study populations, experimental design, and measurement protocols of the BLSA have been previously reported (Shock, 1984; Ferrucci, 2008). The BLSA is a longitudinal cohort study funded and conducted by the NIA Intramural Research Program (IRP). Established in 1958, the BLSA enrolls community-dwelling adults with no major chronic conditions or functional impairments. The GESTALT study is also a study of healthy volunteers, initiated in 2015, and funded and conducted by the NIA IRP. The goal of the BLSA and GESTALT

studies is to evaluate multiple biomarkers related to aging. We note that the inclusion and exclusion criteria for these two studies are essentially identical. Participants underwent testing at the NIA's clinical research unit and were excluded if they had metallic implants, neurologic or medical disorders. Further, all participants underwent a battery of cognitive tests and participants with cognitive impairment were excluded (O'Brien et al., 2009). Clinical and neuropsychological data from participants were reviewed at a consensus conference if they screened positive on the Blessed Information Memory Concentration (BIMC) score (Fuld, 1978) (score ≥ 4), if their Clinical Dementia Rating (CDR) (Morris, 1993) score was ≥ 0.5 using subject or informant report, or if concerns were raised about their cognitive status. The CDR was administered to PET neuroimaging study and autopsy study participants at each visit and to the remaining participants if they scored 4 or more BIMC errors. In addition, all autopsy study participants were evaluated by case conference upon death or withdrawal. Diagnoses of dementia and AD were based on DSM-III-R (American Psychiatric Association, 1994) and the National Institute of Neurological and Communication Disorders and Stroke — AD and Related Disorders Association (McKhann et al., 1984) criteria, respectively. Mild cognitive impairment (MCI) was based on the Petersen criteria (Petersen et al., 1999) and diagnosed when (1) cognitive impairment was evident for a single domain (typically memory) or (2) cognitive impairment in multiple domains occurred without significant functional loss in activities of daily living. The final cohort consisted of 155 cognitively unimpaired volunteers ranging in age from 21 to 94 years (53.3 ± 21.3 years) of which 90 were men (54.9 ± 22.2 years) and 65 were women (52.3 ± 20.0 years), after exclusion of seven participants with cognitive impairment. Age ($p > 0.1$) did not differ significantly between men and women. The number of participants per age-decade was 23 (11 females) within 20–29 years, 22 (7 females) within 30–39 years, 40 (21 females) within 40–49 years, 12 (3 females) within 50–59 years, 10 (6 females) within 60–69 years, 19 (7 females) within 70–79 years, 25 (10 females) within 80–89 years, and 4 (0 females) within 90–99 years. Experimental procedures were performed in compliance with our local Institutional Review Board, and participants provided written informed consent.

Data Acquisition

Magnetic resonance imaging scans were performed on a 3T whole body Philips MRI system (Achieva, Best, Netherlands) using the internal quadrature body coil for transmission and an eight-channel phased-array head coil for reception. For each participant, the imaging protocol for longitudinal and transverse relaxation times (T_1 and T_2), DTI metrics, and CBF imaging was as follow:

T_1 and T_2 Mapping (Bouhrara and Spencer, 2015, 2016, 2017; Bouhrara et al., 2016): 3D spoiled gradient recalled echo (SPGR) images were acquired with flip angles of (2, 4, 6, 8, 10, 12, 14, 16, 18, and 20°), echo time (TE) of 1.37 ms, repetition time (TR) of 5 ms, and acquisition time of ~ 5 min, as well as 3D balanced steady state free precession (bSSFP) images acquired with flip angles of (2, 4, 7, 11, 16, 24, 32, 40, 50, and 60°),

TE of 2.8 ms, TR of 5.8 ms, and acquisition time of ~ 6 min. The bSSFP images were acquired with radiofrequency excitation pulse phase increments of 0 or π in order to account for off-resonance effects (Deoni, 2011). All SPGR and bSSFP images were acquired with an acquisition matrix of $150 \times 130 \times 94$, voxel size of $1.6 \text{ mm} \times 1.6 \text{ mm} \times 1.6 \text{ mm}$. Further, we used the double-angle method (DAM) to correct for excitation radio frequency inhomogeneity (Stollberger and Wach, 1996). For this, two fast spin-echo images were acquired with flip angles of 45° and 90° , TE of 102 ms, TR of 3,000 ms, acquisition voxel size of $2.6 \text{ mm} \times 2.6 \text{ mm} \times 4 \text{ mm}$, and acquisition time of ~ 4 min. All images were acquired with field of view (FoV) of $240 \text{ mm} \times 208 \text{ mm} \times 150 \text{ mm}$. The total acquisition time was ~ 21 min.

Fractional anisotropy (FA) and mean diffusivity (MD) maps were derived from the DTI dataset. DTI protocol consisted of diffusion-weighted images (DWI) acquired with single-shot EPI, TR of 10,000 ms, TE of 70 ms, two b-values of 0 and 700 s/mm^2 , with the latter encoded in 32 directions, acquisition matrix of $120 \times 104 \times 75$, and acquisition voxel size of $2 \text{ mm} \times 2 \text{ mm} \times 2 \text{ mm}$. Two images at $b = 0 \text{ s/mm}^2$ were acquired. Images were acquired with FoV of $240 \text{ mm} \times 208 \text{ mm} \times 150 \text{ mm}$.

Pseudo continuous arterial spin labeling (pCASL) for CBF Mapping (Alsop et al., 2015): 2D control, labeled, and proton density (PD) images were acquired with incorporation of background suppression and single shot-EPI with FoV of $220 \text{ mm} \times 210 \text{ mm} \times 120 \text{ mm}$, spatial resolution of $2.5 \text{ mm} \times 2.5 \text{ mm} \times 5 \text{ mm}$, TE of 15 ms, TR of 7.5 s, labeling duration of 1.8 s, post-labeling delay of 2 s, 30 signal averages, and readout duration of 21.2 ms. The total acquisition time was ~ 12 min.

All images were reconstructed to a voxel size of $1 \text{ mm} \times 1 \text{ mm} \times 1 \text{ mm}$. We emphasize that all MRI studies and ancillary measurements were performed with the same MRI system, running the same pulse sequences, at the same facility, and directed by the same investigators for both BLSA and GESTALT participants.

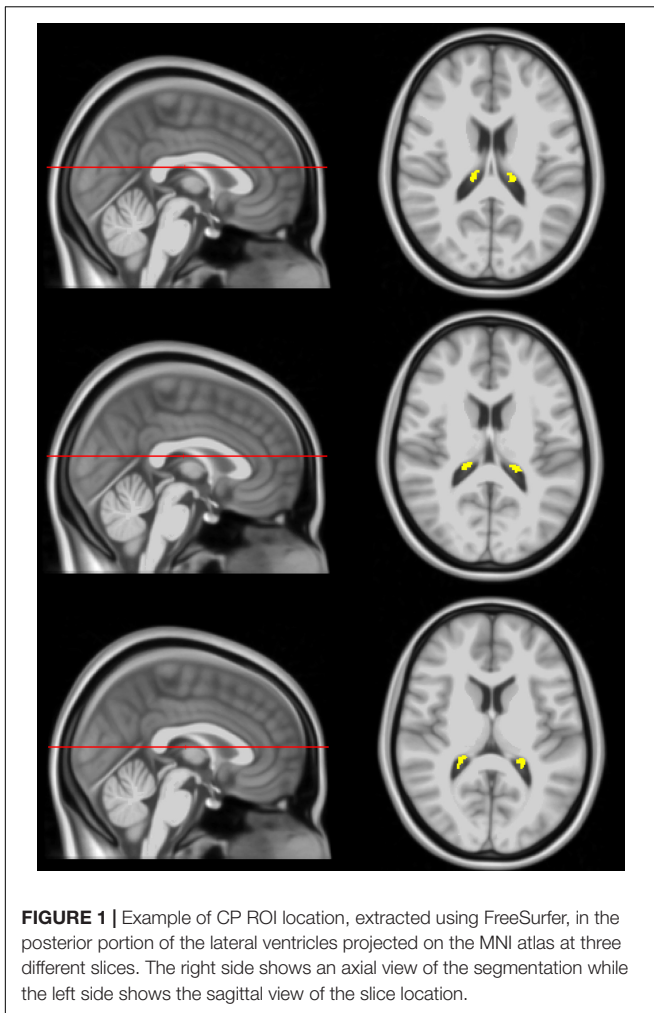
Data Processing

For each participant, the scalp and other non-parenchymal regions within the images were eliminated using the FMRIB Software Library (FSL) using an input image consisting of the SPGR images averaged over all 10 flip angles (Jenkinson et al., 2012); this provides high tissue contrast and signal-to-noise ratio for accurate segmentation.

Choroid Plexus and Lateral Ventricle Volumes Calculation

For each participant, corresponding T_1 -weighted SPGR images were used. Specifically, the FreeSurfer Aseg Atlas (Fischl et al., 2002) was non-linearly registered to the SPGR image averaged over all flip angles using the cortical reconstruction (*recon-all*) pipeline from the FreeSurfer v7.1.1 software¹ (Fischl, 2012). Volumetric measurements were then extracted from the CP and

¹<http://surfer.nmr.mgh.harvard.edu/>



lateral ventricles (LV) regions of interest (ROIs) (**Figure 1**). This method has been used in several other studies indicating reliable CP and LV segmentations (Grech-Sollars et al., 2015; Zhou et al., 2015; Chaddad et al., 2017; Egorova et al., 2019; Lizano et al., 2019; Tadayon et al., 2020). All CP and LV ROIs were thoroughly examined and corrected manually when needed.

Relaxation Times Mapping

Using the FSL software (Jenkinson et al., 2012), all SPGR, bSSFP, and DAM images were linearly registered to the SPGR image acquired at a flip angle of 8° , and the derived transformation matrix was then applied to the original SPGR, bSSFP, and DAM images. Next, a whole-brain T_1 map was generated from the co-registered SPGR dataset using the DESPOT1 analysis and assuming a single relaxing component using the stochastic regions contraction (SRC) algorithm while correcting for transmit field, B_1 , inhomogeneities (Berger and Silverman, 1991; Deoni et al., 2003). The B_1 map was generated from the co-registered fast spin-echo using the DAM approach (Stollberger and Wach, 1996). Further, using these derived T_1 and B_1 maps as input parameters, a whole-brain T_2 map was generated from the co-registered bSSFP dataset using the DESPOT2 analysis

and assuming a single component using the SRC algorithm (Berger and Silverman, 1991; Deoni et al., 2003). B_1 , T_1 , and T_2 maps were generated using in-house MATLAB scripts. All these MATLAB codes are available upon request. Next, using FreeSurfer, the SPGR image averaged over all flip angles for each participant was registered using non-linear registration to FreeSurfer's Aseg atlas and the derived transformation matrix was then applied to the corresponding T_1 and T_2 maps. Finally, the mean T_1 and T_2 values in the CP ROI were calculated.

Fractional Anisotropy and Mean Diffusivity Mapping

The DW images were corrected for eddy current and motion effects using affine registration as implemented in FSL (Jenkinson et al., 2012), and then registered to the DW image obtained with $b = 0 \text{ s/mm}^2$. Moreover, whole-brain FA and MD maps were derived from the co-registered DWI data. Here we used the *DTIfit* tool implemented in FSL to calculate the eigenvalue maps which were used to calculate FA and MD (Basser and Jones, 2002). Then, for each participant, the DW image obtained at $b = 0 \text{ s/mm}^2$ was non-linearly registered to FreeSurfer's Aseg atlas and the calculated matrix of transformation was applied to the corresponding FA and MD maps. Finally, the mean FA and MD values in the CP ROI were calculated.

Cerebral Blood Flow Mapping

For each participant, a whole-brain CBF map was generated from the corresponding pCASL dataset (Alsop et al., 2015). The PD image was non-linearly registered to FreeSurfer's Aseg atlas and the computed transformation matrix was then applied to the corresponding CBF map. Finally, the mean CBF value in the CP ROI was calculated.

Statistical Analysis

The effect of age and sex on T_1 , T_2 , FA, MD, CBF, LV, and CP volume was investigated using multiple linear regression with the mean T_1 , T_2 , FA, MD, CBF, LV, or CP volume value as the dependent variable and sex, age, and age^2 as the independent variables, after mean centering of age. Additionally, the effect of CBF on T_1 , T_2 , FA, or MD was also evaluated using multiple linear regression while accounting for age as a covariate. The threshold for statistical significance was $p < 0.05$. All calculations were performed with MATLAB (MathWorks, Natick, MA, United States).

RESULTS

Figure 2 shows the relationship between the CP volume or the LV volume, after correcting for the total intracranial volume, and age for all participants ($n = 155$). The CP and LV volumes showed significant quadratic effects of age (**Table 1**), age^2 , with both plots showing a non-linear increase in CP or LV volume with age (**Figure 2** and **Table 1**). The effect of sex on the CP and LV volumes was statistically non-significant (**Table 1**).

Figure 3 shows the relaxometry measures, T_1 and T_2 ($n = 146$), the DTI measures, FA and MD ($n = 136$), and CBF ($n = 88$) for all participants within the CP as a function of

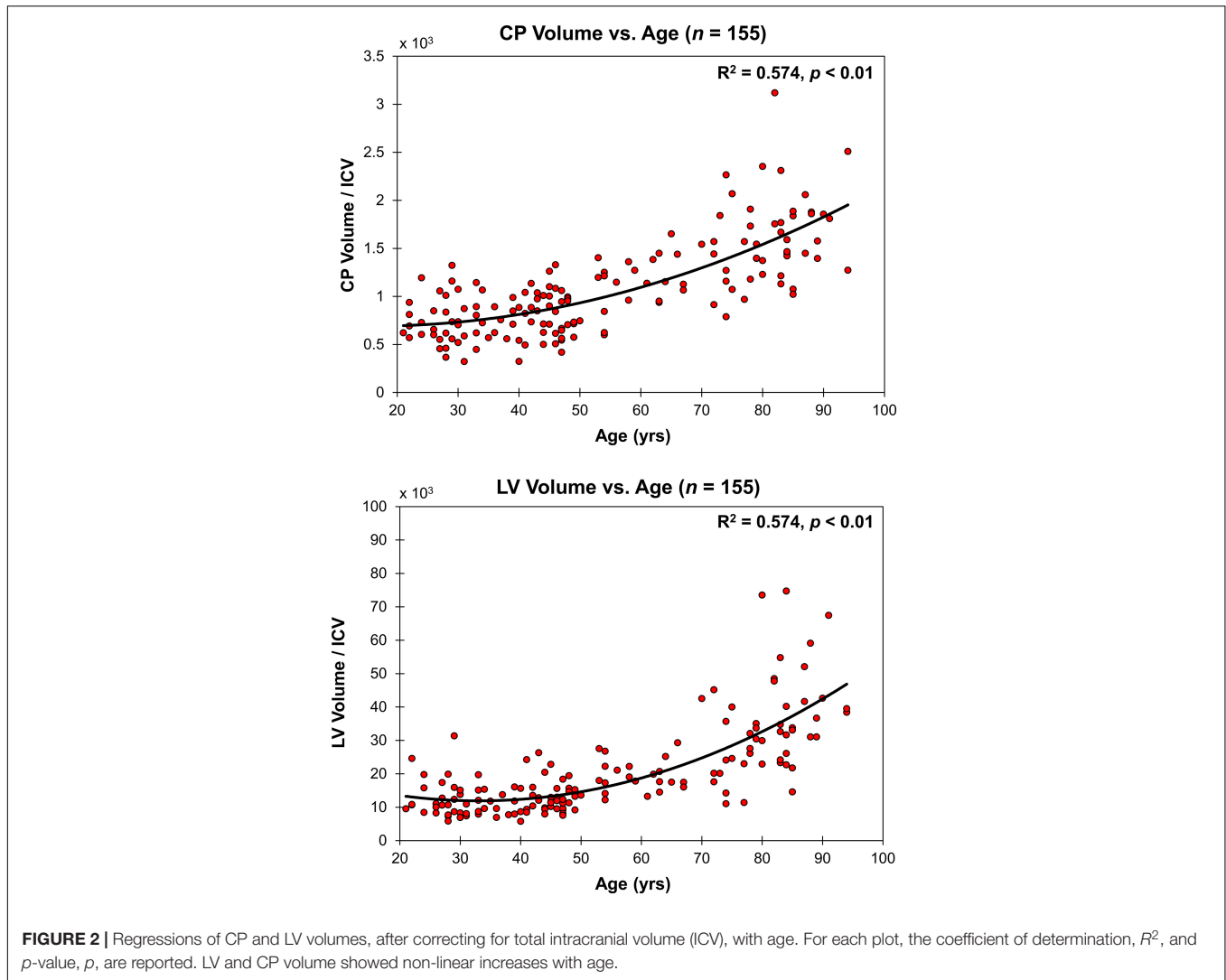


FIGURE 2 | Regressions of CP and LV volumes, after correcting for total intracranial volume (ICV), with age. For each plot, the coefficient of determination, R^2 , and p -value, p , are reported. LV and CP volume showed non-linear increases with age.

TABLE 1 | Coefficients of regression \pm standard error (SE) and p -values of age, age² and sex incorporated in the multiple linear regression analysis for each MR measure.

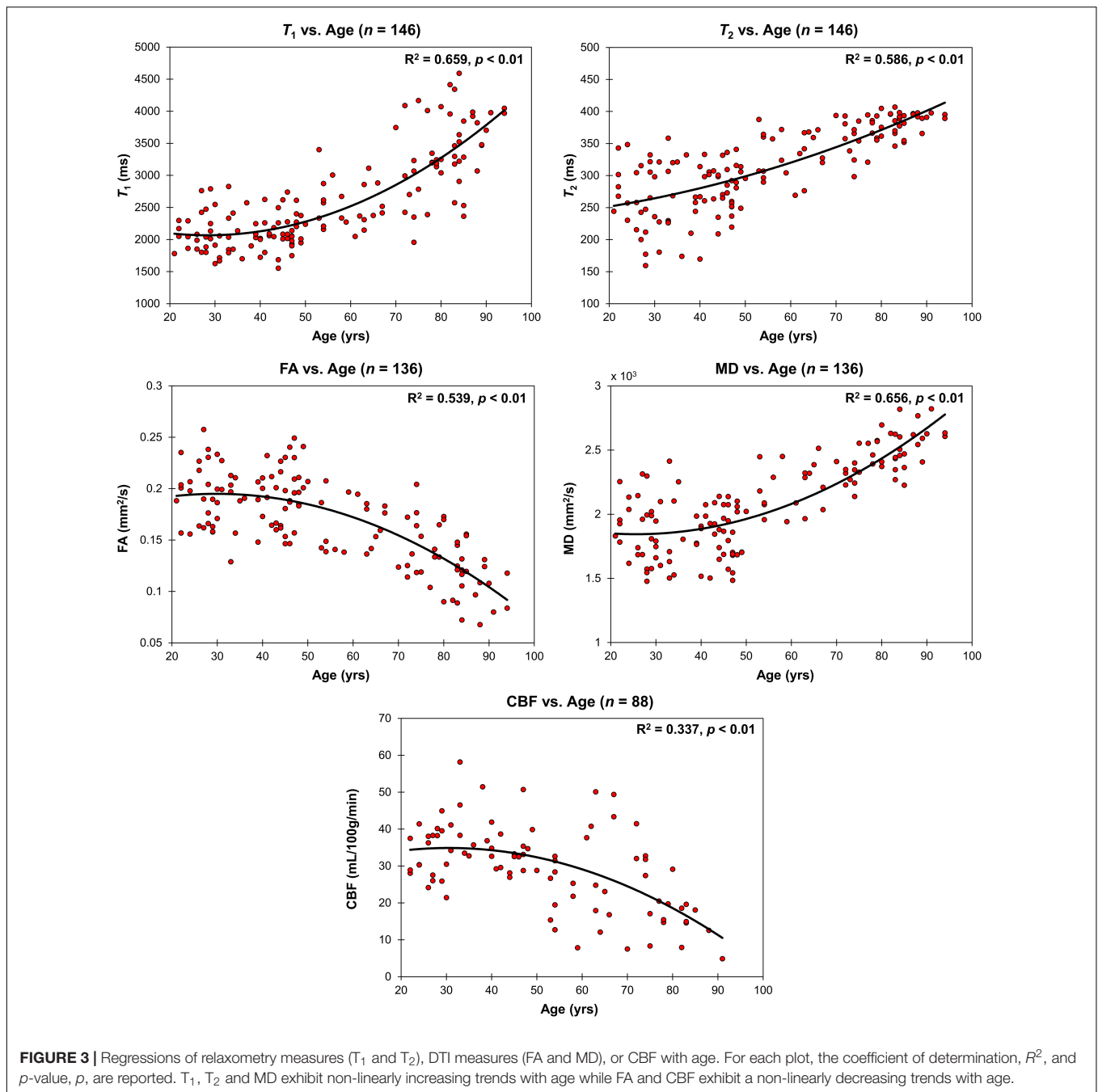
Multiple linear regression model parameters						
	$\beta_{age} \pm SE_{age}$	P_{age}	$\beta_{age^2} \pm SE_{age^2}$	P_{age^2}	$\beta_{sex} \pm SE_{sex}$	P_{sex}
CP volume	$1.56 \times 10^{-5} \pm 1.27 \times 10^{-6}$	<0.01	$1.96 \times 10^{-7} \pm 6.96 \times 10^{-8}$	<0.01	$6.95 \times 10^{-5} \pm 5.19 \times 10^{-5}$	>0.1
LV volume	$3.90 \times 10^{-4} \pm 3.48 \times 10^{-5}$	<0.01	$9.31 \times 10^{-6} \pm 1.91 \times 10^{-6}$	<0.01	$7.07 \times 10^{-4} \pm 1.42 \times 10^{-3}$	>0.1
T_1	23.97 ± 1.69	<0.01	0.45 ± 0.10	<0.01	-17.30 ± 71.21	>0.1
T_2	2.13 ± 0.16	<0.01	$1.44 \times 10^{-2} \pm 8.83 \times 10^{-3}$	>0.1	-2.87 ± 6.68	>0.1
FA	$-1.18 \times 10^{-3} \pm 1.19 \times 10^{-4}$	<0.01	$-2.45 \times 10^{-5} \pm 6.42 \times 10^{-6}$	<0.01	$-4.14 \times 10^{-3} \pm 4.88 \times 10^{-3}$	>0.1
MD	$1.10 \times 10^{-5} \pm 8.58 \times 10^{-7}$	<0.01	$1.86 \times 10^{-7} \pm 4.64 \times 10^{-8}$	<0.01	$9.15 \times 10^{-5} \pm 3.53 \times 10^{-5}$	<0.05
CBF	-0.27 ± 0.05	<0.01	$-6.77 \times 10^{-3} \pm 2.86 \times 10^{-3}$	<0.05	-3.63 ± 2.01	<0.1

Bold indicates $p < 0.05$.

age. Multiple linear regression analysis showed that the effect of age was statistically significant on all of these MRI measures (Table 1). Furthermore, besides T_2 , the quadratic effect of age on all MR measures was statistically significant, with FA ($p < 0.01$) and CBF ($p < 0.05$) exhibiting non-linearly decreasing trends with age, while T_1 ($p < 0.01$) and MD ($p < 0.01$) exhibiting

non-linearly increasing trends with age (Table 1 and Figure 3). Finally, sex effect on MD and CBF was statistically significant, with women exhibiting higher CBF values and lower MD values as compared to men.

Correlations between relaxometry or DTI measures and CBF were assessed using multiple linear regression analyses while



accounting for the effect of age. As shown in **Figure 4** and **Table 2**, CBF was significantly correlated with FA exhibiting a linearly increasing trend with increasing CBF, while T_1 , T_2 , and MD exhibiting linearly decreasing trends with increasing CBF (**Table 2** and **Figure 4**).

DISCUSSION

In this cross-sectional study, we assessed sex and age-related microstructural and functional differences that occur in the CP

using a combination of robust MRI measures in a large cohort of cognitively unimpaired subjects ($n = 155$) spanning 21–94 years of age. We found significant positive association between CP volume and age. We attribute this novel observation to the functional and morphological alterations that occur within the CP as well as to ventriculomegaly and, perhaps, inflamm“aging,” which are common features of normal brain aging. Structurally, the CP is known to undergo numerous changes including accumulation of calcifications and lipofuscin deposits as well as thickening of the stroma (Shuangshoti and Netsky, 1970; Serot et al., 2001; Yalcin et al., 2016). Functionally, CSF

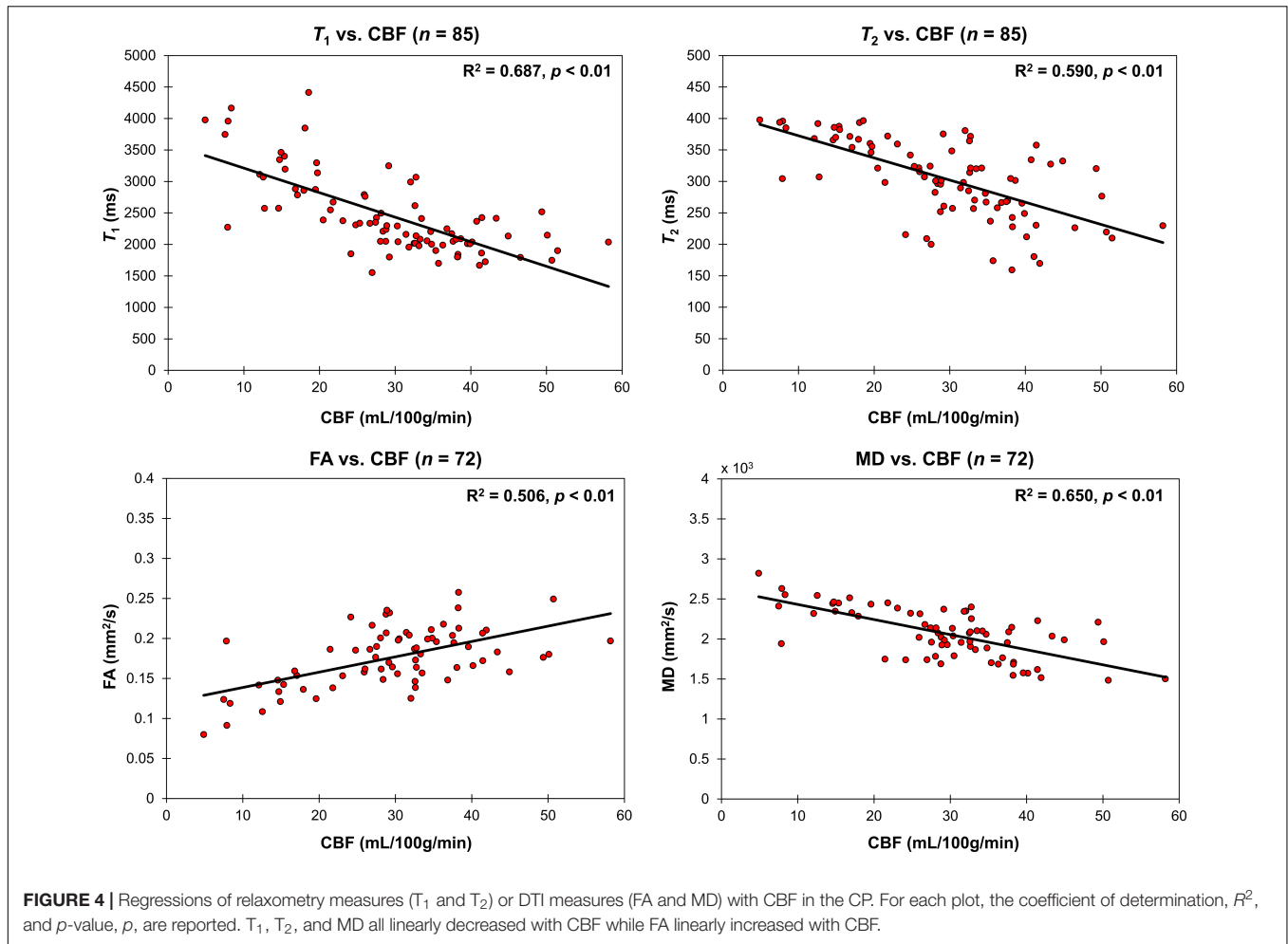


TABLE 2 | Coefficients of regression \pm standard error (SE) and p -values of age, age², and CBF of the multiple linear regression analysis of T_1 , T_2 , FA, or MD.

Multiple linear regression model parameters						
	$\beta_{age} \pm SE_{age}$	p_{age}	$\beta_{age^2} \pm SE_{age^2}$	p_{age^2}	$\beta_{CBF} \pm SE_{CBF}$	p_{CBF}
T_1	14.954 \pm 2.32	<0.01	0.43 \pm 0.12	<0.01	-19.96 \pm 4.53	<0.01
T_2	1.66 \pm 0.26	<0.01	1.27 $\times 10^{-3}$ \pm 1.32 $\times 10^{-3}$	>0.1	-1.83 \pm 0.50	<0.01
FA	-8.53 $\times 10^{-4}$ \pm 2.07 $\times 10^{-4}$	<0.01	-2.06 $\times 10^{-5}$ \pm 1.09 $\times 10^{-5}$	<0.1	1.22 $\times 10^{-3}$ \pm 4.13 $\times 10^{-4}$	<0.01
MD	8.59 $\times 10^{-6}$ \pm 1.40 $\times 10^{-6}$	<0.01	9.28 $\times 10^{-8}$ \pm 7.36 $\times 10^{-8}$	>0.1	-1.41 $\times 10^{-5}$ \pm 2.80 $\times 10^{-6}$	<0.01

Bold indicates $p < 0.05$.

production and turnover decrease with age in the CP (Preston, 2001; Stoquart-ELSankari et al., 2007). Thus, an increase in CP volume may serve as a compensatory or protective mechanism to morphological disruptions and the diminished ability to produce CSF (Redzic et al., 2005). The CP also plays a critical role in producing growth factors (e.g., insulin, IGF1, and IGF2) necessary for normal brain development and regulating its own growth and maintenance of epithelial cell health. While it has been observed that epithelial cell growth of the CP slows with age in younger animals (McDonald and Green, 1988; Liddelow et al., 2010), previous reports have demonstrated that enlarged ventricles and increasing inflammation due to stroke or direct

tissue injury upregulated CP-derived growth factors resulting in volume proliferation of CP epithelial cells (Li et al., 2002; Barkho and Monuki, 2015). Further, previous studies using similar segmentation methods have found a positive association between increasing LV size and CP volume when comparing healthy controls to a disease state (Egorova et al., 2019; Lizano et al., 2019; Tadayon et al., 2020). Due to the multifunctional role of the CP, it is difficult to discern the dominant source and purpose of volume enlargement during normative aging, which necessitates further investigations.

Our finding of higher MD values with age is consistent with Alicioglu et al. (2017). This age-related increase in MD is

further supported by our findings that FA significantly decreased with age and that T_1 and T_2 significantly increased with age. MD describes the overall diffusion and motion of water molecules in the brain, with higher MD values reflect more water mobility (Alexander et al., 2007; Salat, 2014). Similarly, T_1 and T_2 both depend on water content with higher values are also associated with more water mobility (Deoni, 2010). FA, on the other hand, is used to describe anisotropy with low values associated with less restricted movement of molecules (Alexander et al., 2007; Salat, 2014), with lower values of FA with age here are likely due to microstructural alterations or damage to the CP epithelium, leading to increased isotropy of water diffusion. Taken together, we provisionally attribute these observed changes in relaxometry and DTI measures primarily to structural alterations to the CP microstructure and, potentially, to a decreased structural integrity of the BCSFB with advanced age. Indeed, it has been observed in animals that the BCSFB becomes leakier with increasing age, specifically for compounds that were low and medium in molecular weight (Chen et al., 2009). Possible sources for structural alterations in the BCSFB stem from morphological disruptions, as previously described, as well as increasing inflammation. Indeed, previous work showed that aging was associated with a shift toward the Th2 response, which consequently resulted in compromised epithelial tight junctions that are vital in maintaining the structural integrity of the BCSFB (Baruch et al., 2013). However, additional investigations, especially dynamic contrast-enhanced-based measures as well as histological studies, are required to support our conjecture of a potential association between decreased structural integrity of CP and higher BCSFB permeability.

Interestingly, our MD measure exhibited significant differences between men and women, with men exhibiting higher MD values. Alicioglu et al. (2017) observed that women experience a steeper increase in MD after the age of 61 as compared to men. Further, several studies have shown that women exhibit higher CBF as compared to men (Devous et al., 1986; Rodriguez et al., 1988; Podreka et al., 1989; Gur and Gur, 1990; Esposito et al., 1996; Parkes et al., 2004; Liu et al., 2012, 2016; Alisch et al., 2021). Sex differences in CP microstructure and function would be expected. Indeed, in addition to reduced CSF turnover, it is suggested that a dysfunctional BCSFB contributes to greater protein content in the CSF during aging (Chen et al., 2009). In fact, previous reports found that men had a significantly higher CSF/serum albumin ratio (QAlb), a biomarker of BCSFB permeability, compared to women which demonstrates a greater loss of integrity in men (Parrado-Fernandez et al., 2018; Castellazzi et al., 2020). The current scientific literature on sex differences within the CP remain limited, but we speculate that sex hormones may play a role in BCSFB permeability (Santos et al., 2017). Further investigations are required to elucidate sex-related differences in CP's microstructure and function.

We also observed an age-related decrease in CBF in the CP, likely reflecting changes in CP morphology or in the hormonal and neurotransmitter levels. CP blood flow is regulated by several molecules including arginine vasopressin, angiotensin II, dopamine, and serotonin. Arginine vasopressin and angiotensin

II have an inhibitory effect on blood in the CP (Faraci et al., 1988; Maktabi et al., 1990), while dopamine and serotonin are both known to increase blood flow (Townsend et al., 1984; Faraci et al., 1989). Previous studies have showed that aging is associated with increases in arginine vasopressin (Frolkis et al., 2000) and that angiotensin II induces the release of vasopressin (Keil et al., 1975; Qadri et al., 1993), thus indicating a potential mechanism for the age-related decline in CP blood flow. Further, dysfunctional binding and transport of dopamine and serotonin, as observed in other parts of the brain (Meltzer et al., 1998; Karrer et al., 2017), may contribute to decreased CBF. Moreover, morphological examinations show that the arterial walls are thickened and that there is a reduction in blood vessel density during normal aging which leads to limited contact between the blood and the CP epithelial cell layer (Van Cauwenberghe et al., 2020). Finally, our results indicate that CBF was associated with both relaxometry and DTI measures, suggesting that low CBF is associated with the reduced structural integrity of the CP. Indeed, adequate CBF is paramount for nutrient and oxygen delivery and clearance of metabolic by-products; dysfunction of this ability is a characteristic feature of neurodegenerative diseases.

Although we examined a relatively large cohort and used advanced MR methodology, our study has limitations. Our dataset is cross-sectional so that the observed trends in the CP microstructure and function with age as well as the associations between CBF and the other MRI measures requires further validation through longitudinal studies. Such work, motivated by the present results, is underway. Furthermore, our analysis of functional and structural differences in CP with aging were limited to the LVs. We note that CSF partial volume effects may bias derived parameter values. More accurate automated segmentation methods, including the third and fourth ventricles, as well as higher resolution structural images are needed for a better evaluation. In addition, our DTI-related results must be interpreted with caution. Indeed, given the large fraction of free water in the CP, this could have introduced bias in derived parameter values. Although the free-water elimination DTI (FWE-DTI) approach has been used widely to distinguish free-water partial-volume effects from tissue's diffusion in healthy aging and degenerative diseases (Pasternak et al., 2009), it has recently been shown that this method is unstable when applied to single-shell DTI data, requiring careful implementation (Golub et al., 2021). Further, we note that our derived DTI parameters values could change depending on the choice of the b -values. Several DTI protocols involve use of b -values of 0 and 1000 s/mm^2 while others incorporate lower b -values. Our choice of using lower b -values was driven by the desire to minimize non-Gaussian diffusion. Moreover, we used identical ASL experimental parameters for all subjects and acquired CBF images at a single post-labeling delay, implicitly assuming negligible effects of spatial variation in arterial transit time (ATT), the time of the arterial bolus to transit from the labeling plane to the imaging volume (Duvernoy et al., 1981; Qin et al., 2014). Although this is a reasonable assumption (Alsop et al., 2015), ATT may vary spatially and may differ between subjects due to arterial blood velocity differences; this could introduce a small bias in derived CBF values. A multiple

post-labeling delay ASL technique may provide more accurate CBF determination (Qin et al., 2014). Finally, other factors such as inflammatory markers, blood pressure, and medications were not considered in this work.

CONCLUSION

We examined age-related differences in CP microstructure and function in a cohort of cognitively unimpaired participants across a wide age range using quantitative MRI. We showed that aging was associated with increases in volume and decreases in blood flow or structural integrity. This work lay the foundation for further investigation of the functional and structural changes of the CP with normal aging and neuropathology.

DATA AVAILABILITY STATEMENT

The raw data supporting the conclusions of this article will be made available by the authors, without undue reservation.

ETHICS STATEMENT

This study including our MRI protocol was approved by the MedStar Research Institute and the National Institutes of Health Intramural Ethics Committees, and all examinations were

REFERENCES

- Alexander, A. L., Lee, J. E., Lazar, M., and Field, A. S. (2007). Diffusion tensor imaging of the brain. *Neurotherapeutics* 4, 316–329.
- Alicioglu, B., Yilmaz, G., Tosun, O., and Bulakbasi, N. (2017). Diffusion-weighted magnetic resonance imaging in the assessment of choroid plexus aging. *Neuroradiol. J.* 30, 490–495. doi: 10.1177/1971400917714280
- Alisch, J. S. R., Khattar, N., Kim, R. W., Cortina, L. E., Rejimon, A. C., Qian, W., et al. (2021). Sex and age-related differences in cerebral blood flow investigated using pseudo-continuous arterial spin labeling magnetic resonance imaging. *Aging* 13, 4911–4925. doi: 10.18632/aging.202673
- Alsop, D. C., Detre, J. A., Golay, X., Gunther, M., Hendrikse, J., Hernandez-Garcia, L., et al. (2015). Recommended implementation of arterial spin-labeled perfusion MRI for clinical applications: A consensus of the ISMRM perfusion study group and the European consortium for ASL in dementia. *Magn. Reson. Med.* 73, 102–116. doi: 10.1002/mrm.25197
- American Psychiatric Association (1994). *Diagnostic and Statistical Manual of Mental Disorders: DSM-IV*, 4th Edn. Washington, DC: American Psychiatric Association.
- Arnaud, K., and Di Nardo, A. A. (2016). Choroid plexus trophic factors in the developing and adult brain. *Front. Biol.* 11, 214–221. doi: 10.1007/s11515-016-1401-7
- Barkho, B. Z., and Monuki, E. S. (2015). Proliferation of cultured mouse choroid plexus epithelial cells. *PLoS One* 10:e0121738. doi: 10.1371/journal.pone.0121738
- Baruch, K., Ron-Harel, N., Gal, H., Deczkowska, A., Shifrut, E., Ndifon, W., et al. (2013). CNS-specific immunity at the choroid plexus shifts toward destructive Th2 inflammation in brain aging. *Proc. Natl. Acad. Sci. U.S.A.* 110, 2264–2269. doi: 10.1073/pnas.1211270110
- Basser, P. J., and Jones, D. K. (2002). Diffusion-tensor MRI: theory, experimental design and data analysis - a technical review. *NMR Biomed.* 15, 456–467. doi: 10.1002/nbm.783

performed in compliance with the standards established by the National Institutes of Health Institutional Review Board. The patients/participants provided their written informed consent to participate in this study.

AUTHOR CONTRIBUTIONS

JE and MB: research design, results interpretation, and manuscript writing and editing. JA, JE, MK, CT, MA, ZG, and NK: analysis, results interpretation, and manuscript writing and editing. All authors contributed to the article and approved the submitted version.

FUNDING

This work was supported by the Intramural Research Program of the National Institute on Aging of the National Institutes of Health.

ACKNOWLEDGMENTS

We gratefully acknowledge Christopher M. Bergeron, Denise Melvin, and Linda Zukley for their assistance with data acquisition, participant recruitment, and logistics.

- Berger, M. F., and Silverman, H. F. (1991). Microphone array optimization by stochastic region contraction. *Signal Proces. IEEE Trans.* 39, 2377–2386. doi: 10.1109/78.97993
- Bouhrara, M., Reiter, D. A., Celik, H., Fishbein, K. W., Kijowski, R., and Spencer, R. G. (2016). Analysis of mcDESPOT- and CPMG-derived parameter estimates for two-component nonexchanging systems. *Magn. Reson. Med.* 75, 2406–2420.
- Bouhrara, M., and Spencer, R. G. (2015). Incorporation of nonzero echo times in the SPGR and bSSFP signal models used in mcDESPOT. *Magn. Reson. Med.* 74, 1227–1235. doi: 10.1002/mrm.25984
- Bouhrara, M., and Spencer, R. G. (2016). Improved determination of the myelin water fraction in human brain using magnetic resonance imaging through Bayesian analysis of mcDESPOT. *Neuroimage* 127, 456–471. doi: 10.1016/j.neuroimage.2015.10.034
- Bouhrara, M., and Spencer, R. G. (2017). Rapid simultaneous high-resolution mapping of myelin water fraction and relaxation times in human brain using BMC-mcDESPOT. *Neuroimage* 147, 800–811. doi: 10.1016/j.neuroimage.2016.09.064
- Bouzerar, R., Chaarani, B., Gondry-Jouet, C., Zmudka, J., and Baledent, O. (2013). Measurement of choroid plexus perfusion using dynamic susceptibility MR imaging: capillary permeability and age-related changes. *Neuroradiology* 55, 1447–1454. doi: 10.1007/s00234-013-1290-2
- Castellazzi, M., Morotti, A., Tamborino, C., Alessi, F., Pilotto, S., Baldi, E., et al. (2020). Increased age and male sex are independently associated with higher frequency of blood-cerebrospinal fluid barrier dysfunction using the albumin quotient. *Fluids Barriers CNS* 17:14.
- Chaddad, A., Desrosiers, C., and Toews, M. (2017). Multi-scale radiomic analysis of sub-cortical regions in MRI related to autism, gender and age. *Sci. Rep.* 7:45639.
- Chen, R. L., Kassem, N. A., Redzic, Z. B., Chen, C. P., Segal, M. B., and Preston, J. E. (2009). Age-related changes in choroid plexus and blood-cerebrospinal fluid barrier function in the sheep. *Exp. Gerontol.* 44, 289–296. doi: 10.1016/j.exger.2008.12.004
- Chiu, C., Miller, M. C., Caralopoulos, I. N., Worden, M. S., Brinker, T., Gordon, Z. N., et al. (2012). Temporal course of cerebrospinal fluid dynamics and

- amyloid accumulation in the aging rat brain from three to thirty months. *Fluids Barriers CNS* 9:3.
- Cornford, E. M., Varesi, J. B., Hyman, S., Damian, R. T., and Raleigh, M. J. (1997). Mitochondrial content of choroid plexus epithelium. *Exp. Brain Res.* 116, 399–405. doi: 10.1007/pl00005768
- Deoni, S. C. (2010). Quantitative relaxometry of the brain. *Top. Magn. Reson. Imaging* 21, 101–113. doi: 10.1097/rmr.0b013e31821e56d8
- Deoni, S. C. (2011). Correction of main and transmit magnetic field (B0 and B1) inhomogeneity effects in multicomponent-driven equilibrium single-pulse observation of T1 and T2. *Magn. Reson. Med.* 65, 1021–1035. doi: 10.1002/mrm.22685
- Deoni, S. C., Rutt, B. K., and Peters, T. M. (2003). Rapid combined T1 and T2 mapping using gradient recalled acquisition in the steady state. *Magn. Reson. Med.* 49, 515–526. doi: 10.1002/mrm.10407
- Devous, M. D., Stokely, E. M., Chehabi, H. H., and Bonte, F. J. (1986). Normal distribution of regional cerebral blood flow measured by dynamic single-photon emission tomography. *J. Cereb. Blood Flow Metab.* 6, 95–104. doi: 10.1038/jcbfm.1986.12
- Duvernoy, H. M., Delon, S., and Vannson, J. L. (1981). Cortical blood vessels of the human brain. *Brain Res. Bull.* 7, 519–579. doi: 10.1016/0361-9230(81)90007-1
- Egorova, N., Gottlieb, E., Khlif, M. S., Spratt, N. J., and Brodtmann, A. (2019). Choroid plexus volume after stroke. *Int. J. Stroke* 14, 923–930. doi: 10.1177/1747493019851277
- Ennis, S. R., and Keep, R. F. (2006). The effects of cerebral ischemia on the rat choroid plexus. *J. Cereb. Blood Flow Metab.* 26, 675–683. doi: 10.1038/sj.jcbfm.9600224
- Esposito, G., Van Horn, J. D., Weinberger, D. R., and Berman, K. F. (1996). Gender differences in cerebral blood flow as a function of cognitive state with PET. *J. Nucl. Med.* 37, 559–564.
- Evans, P. G., Sokolska, M., Alves, A., Harrison, I. F., Ohene, Y., Nahavandi, P., et al. (2020). Non-invasive MRI of blood-cerebrospinal fluid barrier function. *Nat. Commun.* 11:2081.
- Faraci, F. M., Mayhan, W. G., Farrell, W. J., and Heistad, D. D. (1988). Humoral regulation of blood flow to choroid plexus: role of arginine vasopressin. *Circ. Res.* 63, 373–379. doi: 10.1161/01.res.63.2.373
- Faraci, F. M., Mayhan, W. G., and Heistad, D. D. (1989). Effect of serotonin on blood flow to the choroid plexus. *Brain Res.* 478, 121–126. doi: 10.1016/0006-8993(89)91483-2
- Ferrucci, L. (2008). The Baltimore Longitudinal Study of Aging (BLSA): a 50-year-long journey and plans for the future. *J. Gerontol. A Biol. Sci. Med. Sci.* 63:1416. doi: 10.1093/gerona/63.12.1416
- Fischl, B. (2012). FreeSurfer. *Neuroimage* 62, 774–781. doi: 10.1016/j.neuroimage.2012.01.021
- Fischl, B., Salat, D. H., Busa, E., Albert, M., Dieterich, M., Haselgrove, C., et al. (2002). Whole brain segmentation: automated labeling of neuroanatomical structures in the human brain. *Neuron* 33, 341–355.
- Frolkis, V. V., Kvitnitskaya-Ryzhova, T. Y., and Dubiley, T. A. (2000). Vasopressin, hypothalamo-neurohypophysial system and aging. *Arch. Gerontol. Geriatr.* 29, 193–214. doi: 10.1016/s0167-4943(99)00032-1
- Fuld, P. A. (ed.) (1978). *Psychological Testing in the Differential Diagnosis of the Dementias*. New York, NY: Raven Press.
- Golub, M., Neto Henriques, R., and Gouveia Nunes, R. (2021). Free-water DTI estimates from single b-value data might seem plausible but must be interpreted with care. *Magn. Reson. Med.* 85, 2537–2551. doi: 10.1002/mrm.28599
- Grech-Sollars, M., Hales, P. W., Miyazaki, K., Raschke, F., Rodriguez, D., Wilson, M., et al. (2015). Multi-centre reproducibility of diffusion MRI parameters for clinical sequences in the brain. *NMR Biomed.* 28, 468–485. doi: 10.1002/nbm.3269
- Grieve, S. M., Williams, L. M., Paul, R. H., Clark, C. R., and Gordon, E. (2007). Cognitive aging, executive function, and fractional anisotropy: a diffusion tensor MR imaging study. *Am. J. Neuroradiol.* 28:226.
- Gur, R. E., and Gur, R. C. (1990). Gender differences in regional cerebral blood flow. *Schizophr. Bull.* 16, 247–254. doi: 10.1093/schbul/16.2.247
- Hasan, K. M., Walimuni, I. S., Kramer, L. A., and Frye, R. E. (2010). Human brain atlas-based volumetry and relaxometry: application to healthy development and natural aging. *Magn. Reson. Med.* 64, 1382–1389. doi: 10.1002/mrm.22515
- Hofman, F. M., and Chen, T. C. (2016). “Choroid plexus: structure and function,” in *The Choroid Plexus and Cerebrospinal Fluid*, eds J. Neman and T. C. Chen (Cambridge, MA: Academic Press), 29–40. doi: 10.1016/b978-0-12-801740-1.00003-2
- Hubert, V., Chauveau, F., Dumot, C., Ong, E., Berner, L. P., Canet-Soulas, E., et al. (2019). Clinical imaging of choroid plexus in health and in brain disorders: a mini-review. *Front. Mol. Neurosci.* 12:34. doi: 10.3389/fnmol.2019.00034
- İmamoğlu, H., Erkoç, M. F., Şalk, Y., Okur, A., and Aydemir, E. I. (2013). Evaluation of the normal choroid plexus size in adults with magnetic resonance imaging. *Cumhur. Med. J.* 35, 51–54. doi: 10.7197/1305-0028.1661
- Jenkinson, M., Beckmann, C. F., Behrens, T. E., Woolrich, M. W., and Smith, S. M. (2012). FSL. *Neuroimage* 62, 782–790.
- Joseph-Mathurin, N., Dorieux, O., Trouche, S. G., Boutajangout, A., Kraska, A., Fontes, P., et al. (2013). Amyloid beta immunization worsens iron deposits in the choroid plexus and cerebral microbleeds. *Neurobiol. Aging* 34, 2613–2622. doi: 10.1016/j.neurobiolaging.2013.05.013
- Kadel, K. A., Heistad, D. D., and Faraci, F. M. (1990). Effects of endothelin on blood vessels of the brain and choroid plexus. *Brain Res.* 518, 78–82. doi: 10.1016/0006-8993(90)90956-c
- Karrer, T. M., Josef, A. K., Mata, R., Morris, E. D., and Samanez-Larkin, G. R. (2017). Reduced dopamine receptors and transporters but not synthesis capacity in normal aging adults: a meta-analysis. *Neurobiol. Aging* 57, 36–46. doi: 10.1016/j.neurobiolaging.2017.05.006
- Kaur, C., Rathnasamy, G., and Ling, E. A. (2016). The choroid plexus in healthy and diseased brain. *J. Neuropathol. Exp. Neurol.* 75, 198–213. doi: 10.1093/jnen/nlv030
- Keil, L. C., Summy-Long, J., and Severs, W. B. (1975). Release of vasopressin by angiotensin III. *Endocrinology* 96, 1063–1065. doi: 10.1210/endo-96-4-1063
- Krzyzanowska, A., and Carro, E. (2012). Pathological alteration in the choroid plexus of Alzheimer’s disease: implication for new therapy approaches. *Front. Pharmacol.* 3:75. doi: 10.3389/fphar.2012.00075
- Li, Y., Chen, J., and Chopp, M. (2002). Cell proliferation and differentiation from ependymal, subependymal and choroid plexus cells in response to stroke in rats. *J. Neurol. Sci.* 193, 137–146. doi: 10.1016/s0022-510x(01)00657-8
- Liddel, S. A. (2015). Development of the choroid plexus and blood-CSF barrier. *Front. Neurosci.* 9:32. doi: 10.3389/fnins.2015.00032
- Liddel, S. A., Dziegielewska, K. M., Vandenberg, J. L., and Saunders, N. R. (2010). Development of the lateral ventricular choroid plexus in a marsupial, *Monodelphis domestica*. *Cereb. Fluid Res.* 7:16.
- Liu, W., Lou, X., and Ma, L. (2016). Use of 3D pseudo-continuous arterial spin labeling to characterize sex and age differences in cerebral blood flow. *Neuroradiology* 58, 943–948. doi: 10.1007/s00234-016-1713-y
- Liu, Y., Zhu, X., Feinberg, D., Guenther, M., Gregori, J., Weiner, M. W., et al. (2012). Arterial spin labeling MRI study of age and gender effects on brain perfusion hemodynamics. *Magn. Reson. Med.* 68, 912–922. doi: 10.1002/mrm.23286
- Lizano, P., Lutz, O., Ling, G., Lee, A. M., Eum, S., Bishop, J. R., et al. (2019). Association of choroid plexus enlargement with cognitive, inflammatory, and structural phenotypes across the psychosis spectrum. *Am. J. Psychiatry* 176, 564–572. doi: 10.1176/appi.ajp.2019.18070825
- Lun, M. P., Monuki, E. S., and Lehtinen, M. K. (2015). Development and functions of the choroid plexus-cerebrospinal fluid system. *Nat. Rev. Neurosci.* 16, 445–457. doi: 10.1038/nrn3921
- Madhukar, M., Choudhary, A. K., Boal, D. K., Dias, M. S., and Iantosca, M. R. (2012). Choroid plexus: normal size criteria on neuroimaging. *Surg. Radiol. Anat.* 34, 887–895. doi: 10.1007/s00276-012-0980-5
- Maktabi, M. A., Heistad, D. D., and Faraci, F. M. (1990). Effects of angiotensin II on blood flow to choroid plexus. *Am. J. Physiol. Heart Circ. Physiol.* 258, H414–H418.
- Marques, F., Sousa, J. C., Sousa, N., and Palha, J. A. (2013). Blood-brain-barriers in aging and in Alzheimer’s disease. *Mol. Neurodegen.* 8:38.
- May, C., Kaye, J. A., Atack, J. R., Schapiro, M. B., Friedland, R. P., and Rapoport, S. I. (1990). Cerebrospinal fluid production is reduced in healthy aging. *Neurology* 40:500. doi: 10.1212/wnl.40.3_part_1.500
- Mazucanti, C. H., Liu, Q. R., Lang, D., Huang, N., O’connell, J. F., Camandola, S., et al. (2019). Release of insulin produced by the choroid plexus is regulated by serotonergic signaling. *JCI Insight* 4:e131682.
- McDonald, T. F., and Green, K. (1988). Cell turnover in ciliary epithelium compared to other slow renewing epithelia in the adult mouse. *Curr. Eye Res.* 7, 247–252.

- McKhann, G., Drachman, D., Folstein, M., Katzman, R., Price, D., and Stadlan, E. M. (1984). Clinical diagnosis of Alzheimer's disease: report of the NINCDS-ADRDA work group under the auspices of department of health and human services task force on Alzheimer's disease. *Neurology* 34, 939–944. doi: 10.1212/wnl.34.7.939
- Meltzer, C. C., Smith, G., Dekosky, S. T., Pollock, B. G., Mathis, C. A., Moore, R. Y., et al. (1998). Serotonin in aging, late-life depression, and Alzheimer's disease: the emerging role of functional imaging. *Neuropsychopharmacology* 18, 407–430. doi: 10.1016/s0893-133x(97)00194-2
- Morris, J. C. (1993). The clinical dementia rating (CDR): current version and scoring rules. *Neurology* 43, 2412–2414.
- O'Brien, R. J., Resnick, S. M., Zonderman, A. B., Ferrucci, L., Crain, B. J., Pletnikova, O., et al. (2009). Neuropathologic studies of the Baltimore Longitudinal Study of Aging (BLSA). *J. Alzheimers Dis.* 18, 665–675. doi: 10.3233/jad-2009-1179
- Parkes, L. M., Rashid, W., Chard, D. T., and Tofts, P. S. (2004). Normal cerebral perfusion measurements using arterial spin labeling: reproducibility, stability, and age and gender effects. *Magn. Reson. Med.* 51, 736–743. doi: 10.1002/mrm.20023
- Parrado-Fernandez, C., Blennow, K., Hansson, M., Leoni, V., Cedazo-Minguez, A., and Bjorkhem, I. (2018). Evidence for sex difference in the CSF/plasma albumin ratio in ~20 000 patients and 335 healthy volunteers. *J. Cell. Mol. Med.* 22, 5151–5154. doi: 10.1111/jcmm.13767
- Pasternak, O., Sochen, N., Gur, Y., Intrator, N., and Assaf, Y. (2009). Free water elimination and mapping from diffusion MRI. *Magn. Reson. Med.* 62, 717–730. doi: 10.1002/mrm.22055
- Petersen, R. C., Smith, G. E., Waring, S. C., Ivnik, R. J., Tangalos, E. G., and Kokmen, E. (1999). Mild cognitive impairment: clinical characterization and outcome. *Arch. Neurol.* 56, 303–308. doi: 10.1001/archneur.56.3.303
- Podreka, I., Baumgartner, C., Suess, E., Müller, C., Brücke, T., Lang, W., et al. (1989). Quantification of regional cerebral blood flow with IMP-SPECT. Reproducibility and clinical relevance of flow values. *Stroke* 20, 183–191. doi: 10.1161/01.str.20.2.183
- Preston, J. E. (2001). Ageing choroid plexus-cerebrospinal fluid system. *Microscopy Res. Tech.* 52, 31–37. doi: 10.1002/1097-0029(20010101)52:1<31::aid-jemt5>3.0.co;2-t
- Qadri, F., Culman, J., Veltmar, A., Maas, K., Rascher, W., and Unger, T. (1993). Angiotensin II-induced vasopressin release is mediated through alpha-1 adrenoceptors and angiotensin II AT1 receptors in the supraoptic nucleus. *J. Pharmacol. Exp. Ther.* 267:567.
- Qin, Q., Huang, A. J., Hua, J., Desmond, J. E., Stevens, R. D., and Van Zijl, P. C. (2014). Three-dimensional whole-brain perfusion quantification using pseudo-continuous arterial spin labeling MRI at multiple post-labeling delays: accounting for both arterial transit time and impulse response function. *NMR Biomed.* 27, 116–128. doi: 10.1002/nbm.3040
- Redzic, Z. B., Preston, J. E., Duncan, J. A., Chodobski, A., and Szymdynger-Chodobska, J. (2005). The choroid plexus-cerebrospinal fluid system: from development to aging. *Curr. Top. Dev. Biol.* 71, 1–52. doi: 10.1016/b978-0-12-801740-1.00001-9
- Ricigliano, V., Morena, E., Colombi, A., Tonietto, M., Hamzaoui, M., Poirion, E., et al. (2021). Choroid plexus enlargement characterizes inflammatory multiple sclerosis (2522). *Neurology* 96:2522.
- Rodriguez, G., Warkentin, S., Risberg, J., and Rosadini, G. (1988). Sex differences in regional cerebral blood flow. *J. Cereb. Blood Flow Metab.* 8, 783–789. doi: 10.1038/jcbfm.1988.133
- Salat, D. H. (2014). "Diffusion tensor imaging in the study of aging and age-associated neural disease," in *Diffusion MRI: From Quantitative Measurement to in vivo Neuroanatomy*, 2 Edn, eds H. Johansen-Berg and T. E. J. Behrens (San Diego, CA: Elsevier), 257–281. doi: 10.1016/b978-0-12-396460-1.00012-3
- Santos, C. R., Duarte, A. C., Quintela, T., Tomas, J., Albuquerque, T., Marques, F., et al. (2017). The choroid plexus as a sex hormone target: functional implications. *Front. Neuroendocrinol.* 44, 103–121. doi: 10.1016/j.yfrne.2016.12.002
- Serot, J. M., Béné, M. C., Foliguet, B., and Faure, G. C. (1997). Altered choroid plexus basement membrane and epithelium in late-onset Alzheimer's disease: an ultrastructural study. *Ann. N. Y. Acad. Sci.* 826, 507–509. doi: 10.1111/j.1749-6632.1997.tb48514.x
- Serot, J.-M., Foliguet, B., Béné, M. C., and Faure, G. C. (2001). Choroid plexus and ageing in rats: a morphometric and ultrastructural study. *Eur. J. Neurosci.* 14, 794–798. doi: 10.1046/j.0953-816x.2001.01693.x
- Shock, N. W. (1984). *Normal Human Aging: The Baltimore Longitudinal Study of Aging*. Baltimore, Md: U.S. Dept. of Health and Human Services.
- Shuangshoti, S., and Netsky, M. G. (1970). Human choroid plexus: morphologic and histochemical alterations with age. *Am. J. Anat.* 128, 73–95. doi: 10.1002/aja.1001280107
- Stollberger, R., and Wach, P. (1996). Imaging of the active B1 field in vivo. *Magn. Reson. Med.* 35, 246–251.
- Stoquart-ElSankari, S., Baledent, O., Gondry-Jouet, C., Makki, M., Godefroy, O., and Meyer, M. E. (2007). Aging effects on cerebral blood and cerebrospinal fluid flows. *J. Cereb. Blood Flow Metab.* 27, 1563–1572. doi: 10.1038/sj.jcbfm.9600462
- Tadayon, E., Pascual-Leone, A., Press, D., Santarnecchi, E., and Alzheimer's Disease Neuroimaging Initiative (2020). Choroid plexus volume is associated with levels of CSF proteins: relevance for Alzheimer's and Parkinson's disease. *Neurobiol. Aging* 89, 108–117. doi: 10.1016/j.neurobiolaging.2020.01.005
- Townsend, J. B., Ziedonis, D. M., Bryan, R. M., Brennan, R. W., and Page, R. B. (1984). Choroid plexus blood flow: evidence for dopaminergic influence. *Brain Res.* 290, 165–169. doi: 10.1016/0006-8993(84)90748-0
- Van Cauwenbergh, C., Gorlé, N., and Vandenbroucke, R. E. (2020). "Roles of the choroid plexus in aging," in *Role of the Choroid Plexus in Health and Disease*, eds J. Praetorius, B. Blazer-Yost, and H. Damkier (New York, NY: Springer US), 209–232. doi: 10.1007/978-1-0716-0536-3_9
- Yalcin, A., Ceylan, M., Bayraktutan, O. F., Sonkaya, A. R., and Yuce, I. (2016). Age and gender related prevalence of intracranial calcifications in CT imaging; data from 12,000 healthy subjects. *J. Chem. Neuroanat.* 78, 20–24. doi: 10.1016/j.jchemneu.2016.07.008
- Zhao, L., Taso, M., Dai, W., Press, D. Z., and Alsop, D. C. (2020). Non-invasive measurement of choroid plexus apparent blood flow with arterial spin labeling. *Fluids Barriers CNS* 17:58.
- Zhou, G., Hotta, J., Lehtinen, M. K., Forss, N., and Hari, R. (2015). Enlargement of choroid plexus in complex regional pain syndrome. *Sci. Rep.* 5:14329.

Conflict of Interest: The authors declare that the research was conducted in the absence of any commercial or financial relationships that could be construed as a potential conflict of interest.

Publisher's Note: All claims expressed in this article are solely those of the authors and do not necessarily represent those of their affiliated organizations, or those of the publisher, the editors and the reviewers. Any product that may be evaluated in this article, or claim that may be made by its manufacturer, is not guaranteed or endorsed by the publisher.

Copyright © 2021 Alisch, Kiely, Triebswetter, Alsameen, Gong, Khattar, Egan and Bouhrara. This is an open-access article distributed under the terms of the Creative Commons Attribution License (CC BY). The use, distribution or reproduction in other forums is permitted, provided the original author(s) and the copyright owner(s) are credited and that the original publication in this journal is cited, in accordance with accepted academic practice. No use, distribution or reproduction is permitted which does not comply with these terms.